1521-0111/98/4/454–461$35.00
MOLECULAR PHARMACOLOGY

https://doi.org/10.1124/mol.119.119370
Mol Pharmacol 98:454–461, October 2020

Special Section on 50 Years of Opioid Research

Neprilysin Controls the Synaptic Activity of Neuropeptides in the Intercalated Cells of the Amygdala

G.C. Gregoriou, S.D. Patel, B.L. Winters, and E.E. Bagley

Discipline of Pharmacology & Charles Perkins Centre, Charles Perkins Centre D17, University of Sydney, Camperdown, NSW, Australia

Received December 31, 2019; accepted May 19, 2020

ABSTRACT

Endogenous opioid peptides in the amygdala regulate many of our behaviors and emotional responses. In particular, the endogenous opioid enkephalin plays a significant role in regulating amygdala activity, but its action is strongly limited by peptidases, which degrade enkephalin into inactive fragments. Inhibiting peptidases may be an attractive method to enhance endogenous opioid signaling; however, we do not know which specific peptidase(s) to target. Using inhibition of glutamate release onto the intercalated cells of the amygdala as an assay for enkephalin activity, we applied specific peptidase inhibitors to determine which peptidase(s) regulate enkephalin signaling in this region. Thiorphan (10 μM), captopril (1 μM), or bestatin (10 μM) were used to inhibit the activity of neprilysin, angiotensin-converting enzyme, or aminopeptidase N, respectively. In rat brain slices containing the intercalated cells, we found that inhibition of glutamate release by a submaximal concentration of enkephalin was doubled by application of all three peptidase inhibitors combined. Then, we tested inhibitors individually and found that inhibition of neprilysin alone could enhance enkephalin responses to the same extent as inhibitors of all three peptidases combined. This indicates neprilysin is the predominant peptidase responsible for degrading enkephalins in the intercalated cells of the amygdala. This differs from the striatum, locus coeruleus, and spinal cord, where multiple peptidases metabolize enkephalin. These data highlight the importance of knowing which specific peptidase(s) control opioid actions in the relevant neural circuit and how they change in disease states to allow rational choices of drugs targeting the specific peptidase of interest.

SIGNIFICANCE STATEMENT

Endogenous opioids modulate many of our emotional and behavioral responses. In the amygdala, they modulate our pain, fear, and addictive behaviors. Their actions are terminated when they are catabolized into inactive fragments by at least three different peptidases. In this study, we found that neprilysin selectively controls endogenous opioid concentrations at synapses in the intercalated cells of the amygdala. This peptidase may be a target for regulation of endogenous opioid modulation of amygdala-mediated emotional and behavioral responses.

Introduction

Endogenous opioid peptides in the central nervous system (CNS) modulate a number of complex physiologic and pathophysiological states, including pain perception, fear responses, attachment formation, drug addiction, and decision-making (Lutz and Kieffer, 2013; Bodnar, 2018). Despite this broad influence, the conditions and precise mechanisms in which endogenous opioids regulate synaptic transmission are not well understood. The ability of endogenous opioids to regulate synaptic transmission is determined by a combination of three factors: the level of peptide release, opioid receptor activation, and peptide degradation. The rapid degradation of endogenously released opioids by peptidases contributes to their short-lived biological activity. For example, the enkephalins, an endogenous opioid family with high affinity for μ- and δ-opioid receptors, are rapidly cleaved into inactive peptide fragments in the brain and spinal cord by three main zinc-dependent metallopeptidases (Sullivan et al., 1978; Guyon et al., 1979; Chou et al., 1984; Hiranuma and Oka, 1986; Hiranuma et al., 1997, 1998). Neprilysin (NEP, EC 3.4.24.11) and angiotensin-converting enzyme (ACE, EC 3.4.15.1) cleave enkephalins at a high-affinity site between the glycine-phenylalanine bond (Erdos et al., 1978; Guyon et al., 1979; Hiranuma and Oka,

This work was supported by the National Health and Medical Research Council [Grant APP1047372].
https://doi.org/10.1124/mol.119.119370.

ABBREVIATIONS: ACE, angiotensin-converting enzyme; APN, aminopeptidase N; BLA, basolateral amygdala; CI, confidence interval; CNS, central nervous system; EPSC, excitatory postsynaptic currents; eEPSC, evoked excitatory postsynaptic currents; Im, main island of the intercalated cells; met-enk, methionine enkephalin; NEP, neprilysin; N/OFQ, nociceptin/orphanin FQ; NOP, N/OFQ receptor; PI, peptidase inhibitor; PPR, paired pulse ratio.

1986; Hiranuma et al., 1997, 1998). In contrast, aminopeptidase N (APN, EC 3.4.11.2) cleaves enkephalins at a low-affinity site between the tyrosine-glycine bond (Hersh, 1985, Fig. 1A). Although these biochemical assays have assessed the vulnerability of enkephalin to each peptidase, the ability of each individual peptidase to curtail the cellular actions of enkephalin is not fully defined. In the locus coeruleus, APN and—to a lesser extent—NEP regulate enkephalin activation of G-protein–gated inwardly rectifying potassium channels (Williams et al., 1987), whereas in the spinal cord, the activity of multiple peptidases is required to regulate enkephalin-induced internalization of μ-opioid receptors into spinal cord neurons (Song and Marvizon, 2003). This suggests that even though all three peptidases are expressed widely throughout the central nervous system (Barnes et al., 1988), there may be topographical specificity to peptidase control over endogenous opioid actions.

The amygdala is a brain region that is central to our emotional responses. In particular, the amygdala participates in our learned fear responses, our responses to pain, and aspects of drug addiction (Janak and Tye, 2015), and endogenous opioids regulate all of these responses (Lutz and Kieffer, 2013; Bodnar, 2018). We have recently shown that the endogenous opioid enkephalin inhibits the synaptic inputs and excitability of the main island of the intercalated cells (Im) of the amygdala (Winters et al., 2017). A cocktail of peptidase inhibitors that targeted ACE, APN, and NEP potentiated the actions of endogenous and exogenous enkephalin at glutamatergic synapses in the intercalated cells (Winters et al., 2017). In this exploratory study, we tested the hypothesis that individual peptidases are responsible for enkephalin degradation at this synapse. To test this hypothesis, we used inhibition of glutamatergic synaptic inputs to the intercalated cells as an assay for enkephalin levels to determine how enkephalin levels are changed by application of specific peptidase inhibitors.

Materials and Methods

Animals. All experiments were performed on male Sprague-Dawley rats (3–9 weeks) obtained from the Animal Resources Centre (Government of Western Australia, Perth, Australia). Rats were housed in groups of six in a low–background noise room and maintained on a normal 12-hour light/dark cycle with ad libitum access to food and water. All experimental procedures were approved by the Animal Care Ethics Committee of the University of Sydney (protocols 2017/1257 and 2014/617) and were conducted in accordance with the Australian code of practice for the care and use of animals for scientific purposes.

Slice Preparation. Rats were anesthetized with isoflurane using the open-drop method and then decapitated. The brain was swiftly removed; placed in ice-cold cutting solution of composition (in millimolars) 125 NaCl, 2.5 KCl, 1.25 $NaH_2PO_4.2H_2O$, 2.5 $MgCl_2$, 0.5 $CaCl_2$, 11 D-glucose, and 25 $NaHCO_3$; and saturated with carbogen (95% O_2/5% CO_2). Coronal brain slices (280 μm) containing the rostral amygdala were cut with a vibratome (Leica Biosystems, Nussloch, Germany) and then maintained at 34°C in a chamber containing carbogenated cutting solution. Slices were incubated in this chamber for 1 hour before being used for electrophysiological recordings. For recording, slices were transferred to a recording chamber that was continuously superfused with artificial cerebrospinal fluid containing (in millimolars) 125 NaCl, 2.5 KCl, 1.25 $NaH_2PO_4.2H_2O$, 1 $MgCl_2$, 2 $CaCl_2$, 11 D-glucose, and 25 $NaHCO_3$; saturated with carbogen; and heated to 32–34°C. Neurons of interest were visualized using an upright Olympus BX51 microscope using Dodt gradient contrast optics.

Electrophysiology. Recordings of excitatory postsynaptic currents (EPSCs) were performed using a whole-cell voltage clamp. Neurons were clamped at −70 mV using patch pipettes (3–5 MΩ) containing an internal solution comprising (in millimolars) 140 CsCl, 10 EGTA, 5 HEPES, 2 $CaCl_2$, 2 MgATP, 0.3 NaGTP, and 3 QX314Cl (pH 7.3, 280–285 mOsm/l). EPSCs were evoked via small tungsten bipolar stimulating electrodes (FHC, Bowdoin, ME) placed in the BLA (rate = 0.033–0.050 Hz; stimuli, 0.5–100 V, 100 microseconds). All evoked EPSCs were recorded in the presence of the $GABA_A$ receptor antagonists SR-95531 (10 μM) and picrotoxin (100 μM) to block fast inhibitory synaptic transmission.

Data Collection and Analysis. All recorded signals were amplified, low-pass filtered (5 kHz), digitized, and acquired (sampled at 10 kHz) using Multiclamp 700B amplifier (Molecular Devices), and online/off-line analysis was performed with Axograph Acquisition software (Molecular Devices). In all experiments, series resistance was monitored, and cells were discarded if resistance was >20 MΩ or fluctuated by more than 20%. The number of experiments was not planned before any data were obtained; thus, the current study is of an exploratory nature. For this type of experiment, we would typically obtain n = 5–7, but numbers may vary because of effect size or variability. In addition, some control experiments have higher replicates. As follows, the data analysis was preplanned. All evoked excitatory postsynaptic currents (eEPSCs) were analyzed with respect to peak amplitude. Peak amplitude was quantified as the mean peak amplitude of four to eight eEPSCs after responses reached a stable plateau. Paired pulse ratio (PPR) was calculated from the peak amplitudes of eEPSCs elicited by paired stimulating pulses (50-millisecond interpulse interval, second eEPSC/first eEPSC). Effects of exogenously applied drugs are represented as percent inhibition, which reflects the difference between mean amplitude during drug superfusion and baseline. Reversal of drug effects by antagonists was calculated as the proportion of the baseline amplitude recovered during the washout or antagonist application over the total eEPSC amplitude lost during drug superfusion. No outliers were removed from analysis.

Statistical analysis was determined before any results were obtained. Statistical analysis was performed using Prism (GraphPad Software, San Diego, CA). Results were analyzed as follows. Differences between individual drug effects and baseline were analyzed using unpaired Student's t tests. Drug effects within the same cells were analyzed using paired Student's t tests. The difference between drug effects with respect to baseline was analyzed using one-way repeated measures ANOVAs followed by Bonferroni tests for multiple comparisons. All statistical tests and results are indicated in the figure legends. P values <0.05 were regarded as significant. Data are expressed as means ± S.D. or, when expressed as percent inhibition, are shown as means with lower-upper 95% confidence interval (CI) of the mean.

Drugs. All drugs were diluted to their final concentration in artificial cerebrospinal fluid and applied by superfusion. Concentrations of 6-imino-3-(4-methoxyphenyl)-1(6*H*)-pyridazine butanoic acid hydrobromide (SR-95531; 10 μM; Abcam, Cambridge, UK), picrotoxin (100 μM; Sigma, St. Louis, MO), methionine-enkephalin (met-enk; 100 nM; Sigma), naloxone (10 μM; Tocris, Bristol, UK), thiorphan (10 μM; Abcam), bestatin (10 μM; Abcam), captopril (1 μM; Sigma), and (±)-1-[(3*R**,4*R**)-1-(cyclooctylmethyl)-3-(hydroxymethyl)-4-piperidinyl]-3-ethyl-1,3-dihydro-2*H*-benzimidazol-2-one (J113397; 1 μM; Tocris) remained the same for all experiments. Nociceptin/orphanin FQ (N/OFQ; 100, 300 nM, 1, 3 μM; Tocris) concentration was varied where indicated.

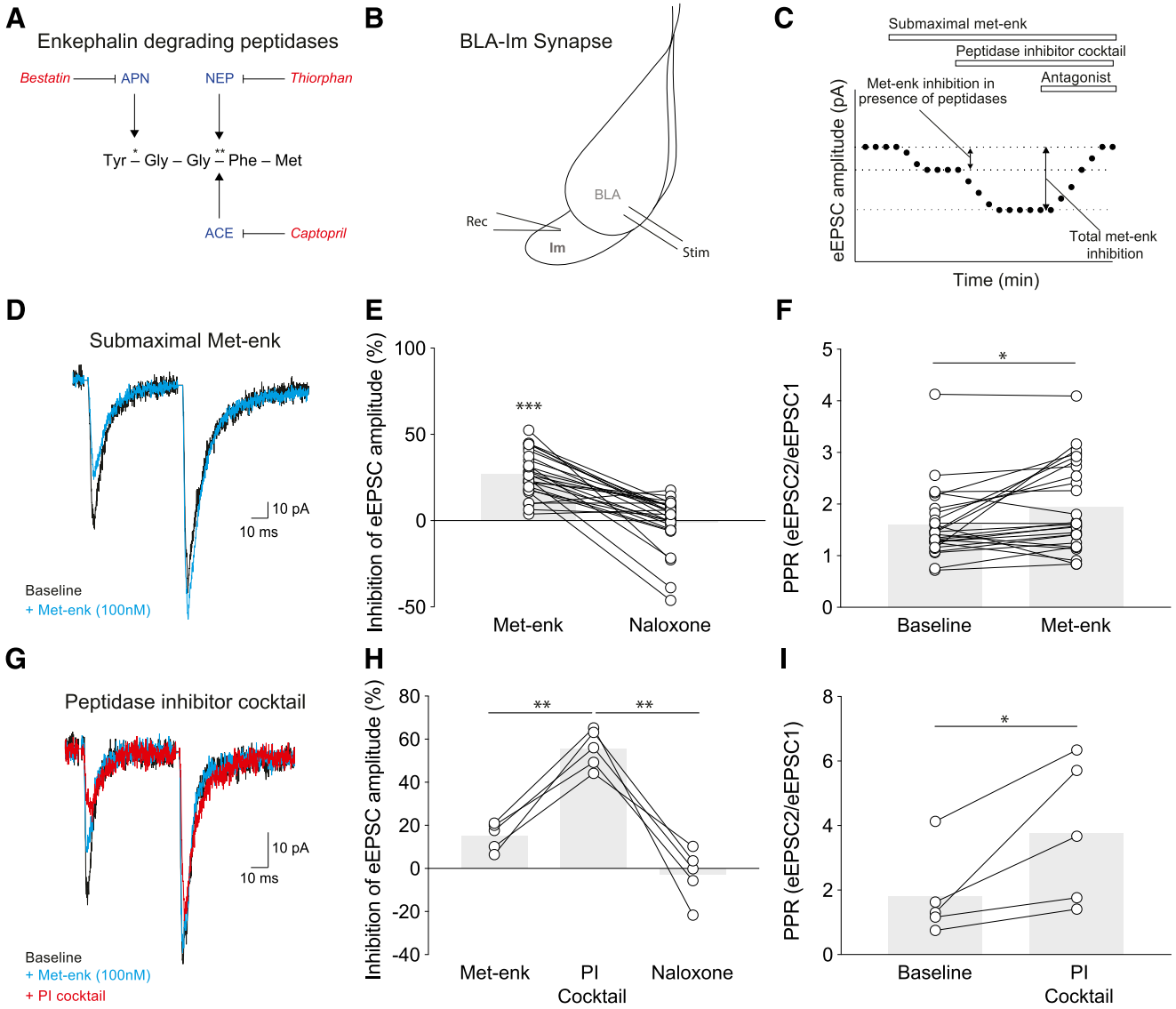

Fig. 1. The inhibition of glutamate transmission produced by met-enk at the BLA-Im synapse is enhanced by inhibiting enkephalin-degrading peptidases. (A) Met-enk is catabolized by various peptidases. The diagram shows low-affinity cleavage site (*), high-affinity cleavage site (**), peptidases in blue (APN, NEP, ACE), and their corresponding inhibitors in red. (B) Schematic of BLA-Im stimulation and recording sites. Bipolar stimulating electrodes were placed in the BLA, and the response of Im neurons to this stimulation (stim) was recorded (rec). (C) Graphic showing experimental paradigm. (D) Representative traces showing inhibition of baseline eEPSC amplitude by submaximal met-enk (100 nM). (E) Graph showing percent inhibition of eEPSC amplitude (from baseline) by submaximal met-enk (100 nM) and reversal by naloxone (10 μM). ***$P < 0.001$, met-enk vs. baseline, unpaired t test. (F) Before and after scatter plot of PPR at baseline and submaximal met-enk (100 nM). *$P = 0.011$, baseline vs. met-enk, paired t test. (G) Representative traces showing that inhibition of baseline eEPSC amplitude by submaximal met-enk (100 nM) is potentiated by a cocktail of peptidase inhibitors (PI cocktail: thiorphan 10 μM, bestatin 10 μM, and captopril 1 μM). (H) Graph showing percent inhibition of eEPSC amplitude (from baseline) by submaximal met-enk (100 nM), PI cocktail (thiorphan 10 μM, bestatin 10 μM, and captopril 1 μM), and reversal by naloxone (10 μM). **$P = 0.0031$, met-enk vs. PI cocktail, one-way repeated measures ANOVA followed by Bonferroni multiple comparisons test; **$P = 0.0070$, PI cocktail vs. naloxone, one-way repeated measures ANOVA followed by Bonferroni multiple comparisons test. (I) Before and after scatter plot of PPR at baseline and during PI cocktail (thiorphan 10 μM, bestatin 10 μM, and captopril 1 μM). *$P = 0.0457$, baseline vs. PI cocktail, paired t test. Each point on the graphs represents a single neuron. Bars on graphs represent the means.

Results

Enkephalin-Degrading Peptidases Control met-enk Actions at the BLA-Im Synapse. In the current paper, we indirectly measured peptidase activity to determine the level of control they exert over opioid activity at the BLA (basolateral amygdala)-Im synapse. By electrically stimulating the BLA, we recorded the resulting eEPSCs from Im neurons using whole-cell patch-clamp electrophysiology (Fig. 1B). Then, by applying a cocktail of enkephalin-degrading peptidase inhibitors (PI cocktail) to our slices, we were able to examine the extent to which these peptidases collectively regulate enkephalin activity. Our PI cocktail consisted of thiorphan (10 μM), captopril (1 μM), and bestatin (10 μM), which respectively inhibit NEP (Roques et al., 1980, Rose et al., 2002, Table 1), ACE (Dalkas et al., 2010), and APN (Rich et al., 1984; Fig. 1A; Table 1). The concentration of thiorphan was chosen to inhibit both isoforms of NEP (Table 1). Although thiorphan and captopril have been reported to display inhibitory activity at other peptidases, they are most selective

TABLE 1
Selectivity of peptidase inhibitors

Inhibitor	Peptidase Source	NEP	NEP1	NEP2	APN	ACE	Reference
Thiorphan	Striatal membranes	4.7 nM				150 nM	Roques et al., 1980
	Not stated	4 nM				>100 nM	Inguimbert et al., 2002
	Expressed human		6.9 nM	22 μM			Whyteside and Turner, 2008
	Expressed rat	4 nM		120–250 nM			Rose et al., 2002
	Porcine basilar artery	1.4 nM				295 nM	Miyamoto et al., 2002
Bestatin	Brain membranes				0.5–4μM		Gros et al., 1985
	Porcine kidney				4.1 μM		Rich et al., 1984
Captopril	Striatal membranes	10 μM				7 nM	Roques et al., 1980
	Expressed human					6.3 nM	Dalkas et al., 2010
	Porcine basilar artery					38 nM	Miyamoto et al., 2002
	Not stated	>1000 nM				2 nM	Inguimbert et al., 2002

for our peptidases of interest (Table 1). Thus, thiorphan- and captopril-sensitive responses could be predominately attributable to NEP and ACE. In these experiments, a submaximal concentration of met-enk was chosen so that if peptidase inhibition increased extracellular met-enk concentrations, we could observe the resulting increase in synaptic inhibition (Fig. 1C). At the BLA-Im synapse, a submaximal concentration of met-enk (100 nM) modestly, yet consistently, inhibits baseline eEPSC amplitude (baseline: 107.61 ± 63.64 pA vs. met-enk: 80.39 ± 52.26 pA, $P < 0.0001$, paired Student's t test, Fig. 1, D and E). This inhibition was accompanied by an increase in paired pulse ratio, indicating a presynaptic site of met-enk action (baseline: 1.59 ± 0.68 vs. met-enk: 1.94 ± 0.87, $P = 0.0107$, paired Student's t test, Fig. 1F). Application of the PI cocktail significantly enhances the ability of submaximal met-enk to inhibit eEPSC amplitude (met-enk: 15.04%, 95% CI 7.06–23.02, met-enk + PI cocktail: 55.57%, 95% CI 44.41–66.74, met-enk + PI cocktail + naloxone: −2.73%, 95% CI −17.71 to 12.26, $P < 0.01$, one-way ANOVA, Fig. 1, G and H), with an increase in paired pulse ratio also being observed during inhibitor application (baseline: 1.80 ± 1.34 vs. PI cocktail: 3.78 ± 2.23, $P < 0.05$, paired Student's t test, Fig. 1I). The findings are consistent with our previous data (Winters et al., 2017), which show enhanced opioid inhibition of synaptic transmission at the BLA-Im synapse after pharmacological inhibition of the three enkephalin-degrading peptidases.

Paired pulse stimulation of the BLA releases endogenous opioids in the Im; however, the amount of peptide released by this low stimulation is too rapidly degraded to exert any measurable effect (Winters et al., 2017). Thus, we administered the PI cocktail to the BLA-Im synapse alone to see whether we could protect endogenous opioids from degradation and observe their activity. When the PI cocktail was applied to slices in the absence of met-enk, it had little effect on baseline synaptic transmission (baseline: 155.44 ± 72.03 pA, $n = 7$ vs. PI cocktail 139.24 ± 80.72 pA, $n = 7$, inhibition = 12.92%, 95% CI −0.20 to 26.05, paired Student's t test, $P = 0.14$). This suggests that any further increase to the level of met-enk inhibition by the PI cocktail can be interpreted as being predominately due to protection of exogenous met-enk from degradation.

NEP Is the Critical Enkephalin-Degrading Peptidase at the BLA-Im Synapse. Although all three of the enkephalin-degrading peptidases are expressed in the amygdala (Pollard et al., 1989; Krizanova et al., 2001; Banegas et al., 2005), it is unknown which specific peptidase is crucial for met-enk degradation at the BLA-Im synapse. Thus, we sought to determine the relative contribution of enkephalin-degrading peptidases to the prevention of enkephalinergic signaling through opioid receptors at the BLA-Im synapse by testing each peptidase inhibitor individually. Figure 2 shows that the application of 1 μM captopril (Fig. 2, A–C) or 10 μM bestatin (Fig. 2, D–F) provided met-enk with no protection against peptidase degradation. The addition of 10 μM thiorphan, however, significantly increased the extent of met-enk inhibition (met-enk: 28.65%, 95% CI 13.87–43.44, met-enk + thiorphan: 55.80%, 95% CI 46.15–65.44, met-enk + thiorphan + naloxone: 8.13%, 95% CI −0.65 to 16.91, $P < 0.05$, one-way ANOVA, Fig. 2, G–I). Moreover, this enhanced inhibition was comparable to that observed with the combined application of all three peptidases (PI cocktail: 55.57%, 95% CI 46.15–65.44, $n = 5$ vs. thiorphan alone: 55.80%, 95% CI 44.41–66.74, $n = 6$, $P = 0.97$, unpaired Student's t test), suggesting that met-enk was protected from peptidase breakdown to a similar degree. Together, these results indicate that the peptidase targeted by thiorphan (NEP) is both necessary and sufficient for substantial met-enk degradation at the BLA-Im synapse.

NEP Regulation of Synaptic Transmission at the BLA-Im Traverses Peptide Systems. Although NEP has been termed an enkephalinase and changes in NEP activity can increase and/or decrease enkephalin levels to the extent that endogenous opioid-related behaviors such as pain responses, behavioral despair, and conditioned reinforcement are altered (Schwartz et al., 1985), NEP is not exclusively selective for enkephalin. In fact, NEP has a wide anatomic distribution (Bayes-Genis et al., 2016) and a broad substrate selectivity and can cleave various peptide targets including, but not limited to, tachykinins (Matsas et al., 1983), neurotensin (Kitabgi et al., 1992), natriuretic peptides (Schwartz et al., 1990), and cholecystokinin (Matsas et al., 1984). One such candidate substrate is N/OFQ—an opioid-like neuropeptide with some sequence similarity to the endogenous opioid dynorphin. Like endogenous opioids, N/OFQ has a glycine-phenylalanine bond, is degraded by NEP in membrane fragments (Sakurada et al., 2002), and is expressed in the amygdala (Neal et al., 1999). We took advantage of these parallels to investigate whether NEP regulation of peptide activity at the BLA-Im synapse was restricted to opioids or whether it would extend to regulation of other neuropeptides. First, we determined the effect of N/OFQ on glutamate release at the BLA-Im. We found that in untreated tissue, N/OFQ produced a concentration-dependent inhibition of eEPSCs (Fig. 3A). At the maximal concentration, N/OFQ inhibition was accompanied by an increase in PPR; however, this was not observed at lower concentrations (baseline: 1.02 ± 0.13, N/OFQ: 1.33 ± 0.21, $P < 0.05$, paired Student's t test,

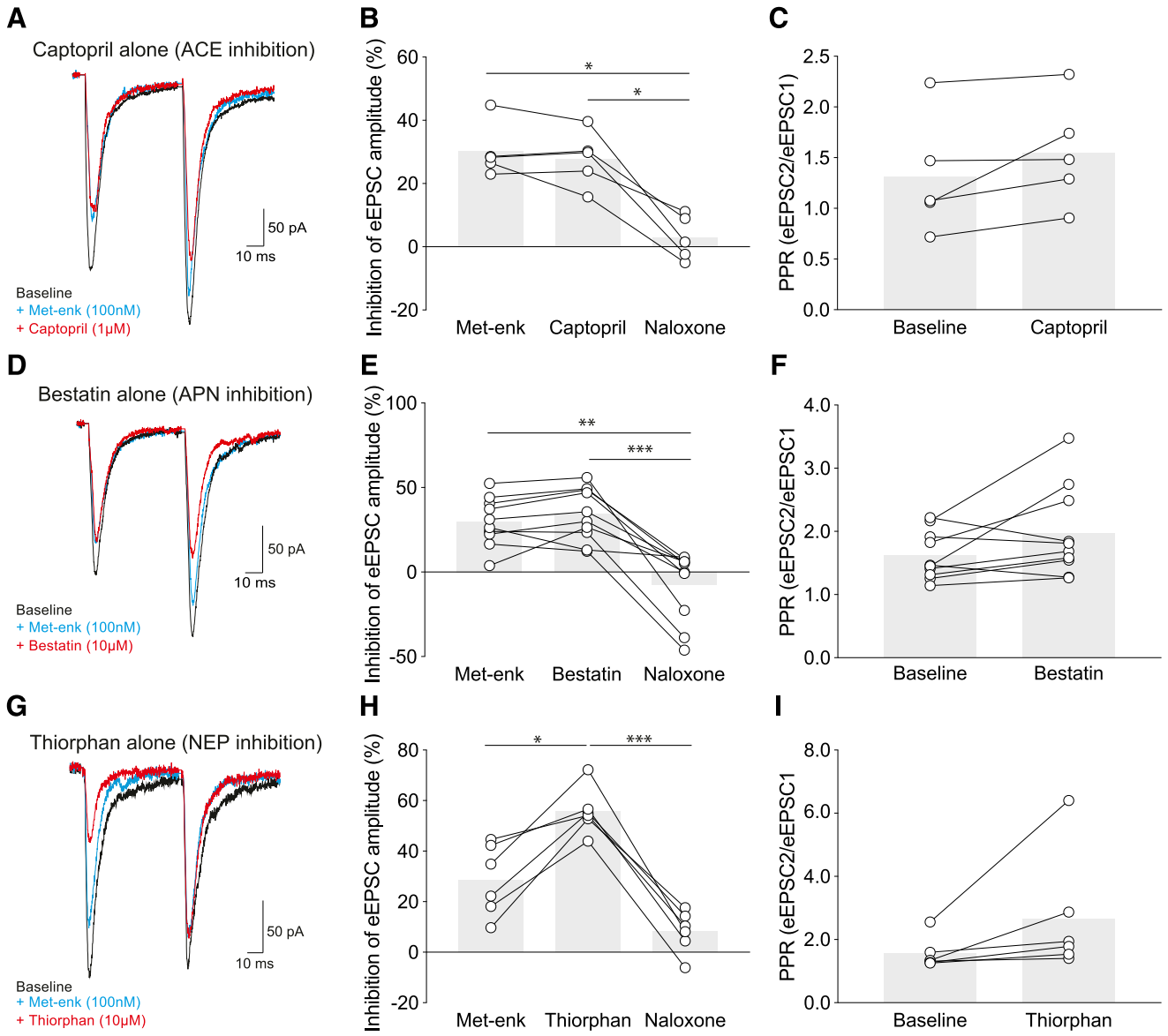

Fig. 2. Effect of individual peptidase inhibitors on met-enk–induced inhibition of glutamate neurotransmission. (A) Representative traces showing baseline amplitude of eEPSC at BLA-Im synapse and inhibition of baseline amplitude after application of submaximal met-enk (100 nM) and then captopril (1 μM). (B) Graph showing percent inhibition of eEPSC amplitude (from baseline) by submaximal met-enk (100 nM), captopril (1 μM), and reversal by naloxone (10 μM). *P = 0.0217, met-enk vs. naloxone, one-way repeated measures ANOVA followed by Bonferroni multiple comparisons test; *P = 0.0154, captopril vs. naloxone, one-way repeated measures ANOVA followed by Bonferroni multiple comparisons test. (C) Before and after scatter plot of PPR in baseline and captopril. Captopril did not change the PPR. P = 0.1144, paired t test. (D) Representative traces showing baseline amplitude of eEPSC at BLA-Im synapse and inhibition of baseline amplitude after application of submaximal met-enk (100 nM) and then bestatin (10 μM). (E) Graph showing percent inhibition of eEPSC amplitude (from baseline) by submaximal met-enk (100 nM), bestatin (10 μM), and reversal by naloxone (10 μM). **P = 0.0023, met-enk vs. naloxone, one-way repeated measures ANOVA followed by Bonferroni multiple comparisons test; ***P = 0.0006, bestatin vs. naloxone, one-way repeated measures ANOVA followed by Bonferroni multiple comparisons test. (F) Before and after scatter plot of PPR in baseline and bestatin. Bestatin did not change the PPR. P = 0.0835, paired t test. (G) Representative traces showing baseline amplitude of eEPSC at BLA-Im synapse and inhibition of baseline amplitude after application of submaximal met-enk (100 nM) and then thiorphan (10 μM). (H) Graph showing percent inhibition of eEPSC amplitude (from baseline) by submaximal met-enk (100 nM), thiorphan (10 μM), and reversal by naloxone (10 μM). *P = 0.118, met-enk vs. thiorphan, one-way repeated measures ANOVA followed by Bonferroni multiple comparisons test; ***P = 0.0003, thiorphan vs. naloxone, one-way repeated measures ANOVA followed by Bonferroni multiple comparisons test. (I) Before and after scatter plot of PPR in baseline and thiorphan. Thiorphan did not change the PPR. P = 0.1201, paired t test. Each point on the graphs represents a single neuron. Bars on graphs represent means.

Fig. 3B). The N/OFQ inhibition of eEPSC amplitude was reversed by the N/OFQ receptor antagonist J113397 (Fig. 3D). These data indicate that, in a manner analogous to endogenous opioids, the BLA-Im synapse is regulated by N/OFQ.

By taking advantage of our established submaximal N/OFQ concentration (100 nM) and then applying thiorphan (10 μM) to slices, we tested whether NEP could also regulate N/OFQ signaling at the BLA-Im synapse. In all cells, the submaximal N/OFQ inhibition was enhanced after thiorphan application (N/OFQ: 17.04%, 95% CI 1.21–32.88, N/OFQ + thiorphan: 28.98%, 95% CI 13.54–44.43, N/OFQ + thiorphan + J113397: 2.97%, 95% CI −2.23 to 8.17, $P < 0.05$, one-way ANOVA, Fig. 3, C and D). However, unlike met-enk, thiorphan application did not change PPR (Fig. 3E).

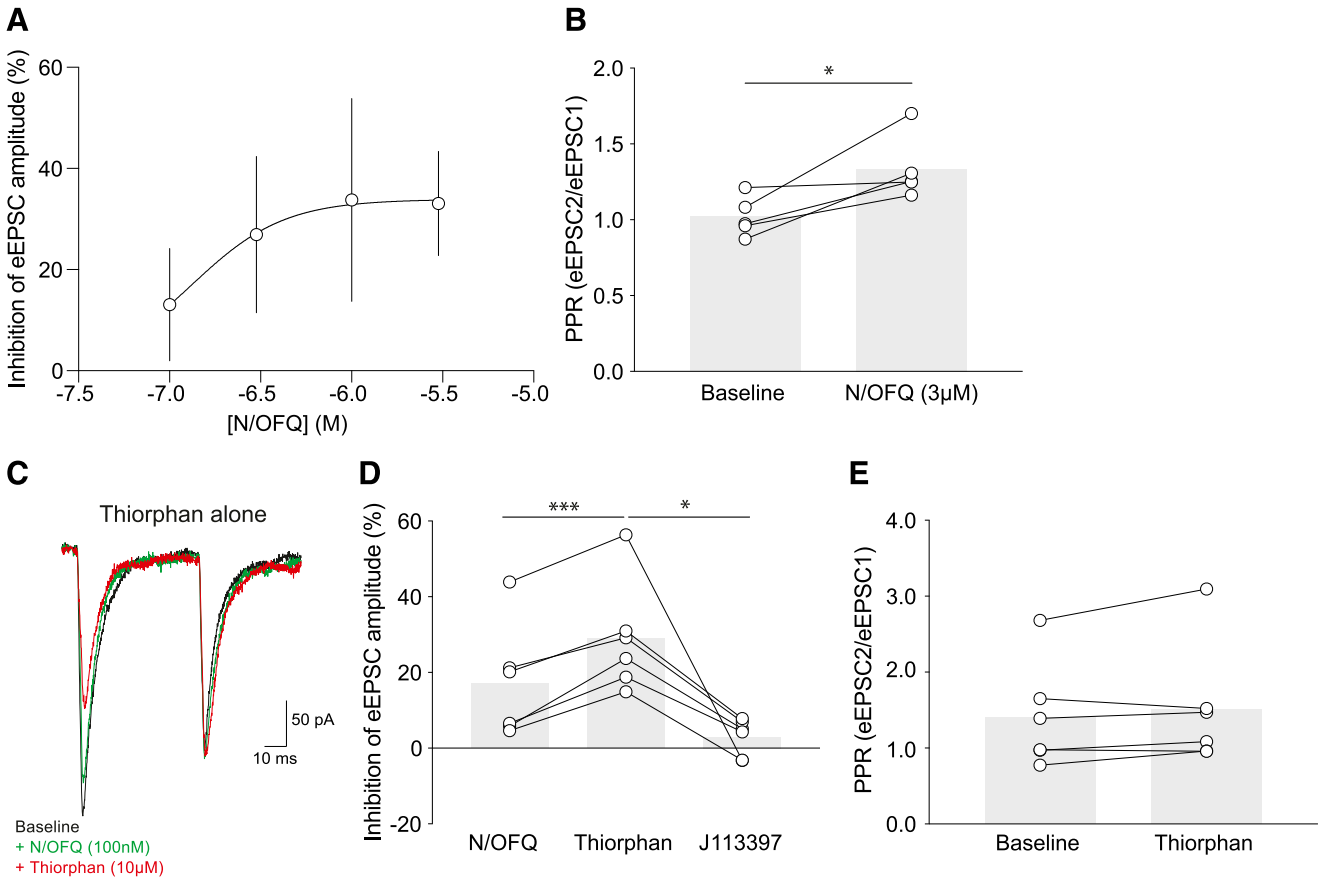

Fig. 3. Neprilysin blockade enhances actions of nociceptin at the BLA-Im synapse. (A) Concentration-response relationship for percent inhibition of eEPSC amplitudes by N/OFQ at the BLA-Im synapse. Each point shows the mean ±95% CI of five neurons. A logistic function was fitted to the concentration-response curve. (B) Before and after scatter plot of PPR in baseline and maximal N/OFQ (3 μM). *P = 0.0345, baseline vs. N/OFQ (3 μM), paired t test. (C) Representative traces showing baseline amplitude of eEPSC at BLA-Im synapse and inhibition of baseline amplitude after application of submaximal N/OFQ (100 nM) and then thiorphan (10 μM). (D) Graph showing percent inhibition of eEPSC amplitude (from baseline) by submaximal N/OFQ (100 nM), thiorphan (10 μM), and reversal by the selective N/OFQ receptor (NOP) \ antagonist J113397 (1 μM). ***P = 0.0010, N/OFQ vs. thiorphan, one-way repeated measures ANOVA followed by Bonferroni multiple comparisons test; *P = 0.0376, thiorphan vs. J113397, one-way repeated measures ANOVA followed by Bonferroni multiple comparisons test. (E) Before and after scatter plot of PPR in baseline and thiorphan (10 μM). Thiorphan did not change the PPR. P = 0.2177, paired t test. Each point on the graphs represents a single neuron. Bars on graphs represent means.

Together these data indicate that NEP also targets N/OFQ for degradation in the intercalated cells of the amygdala.

Discussion

The present results demonstrate that peptidase degradation of met-enk limits the extent of opioid inhibition of synaptic glutamate release to the intercalated cells of the amygdala. We tested inhibitors of the three main classes of enkephalin-degrading peptidases and found that inhibition of NEP alone could enhance enkephalin responses to the same extent as inhibitors of all three peptidases combined. The potentiation of opioid inhibition in intercalated cells by thiorphan alone indicates that inhibition of NEP prevents cleavage of the Gly-Phe bond, which is sufficient to protect enkephalin from degradation. The failure of bestatin and captopril to alter the level of met-enk inhibition suggests that neither APN nor ACE activity can sufficiently change enkephalin concentrations at synaptic opioid receptors enough to alter glutamate release.

The current results, indicating the dominance of NEP in metabolism of enkephalins in the intercalated cells, differ not only from the multiple peptidases responsible for enkephalin metabolism in in vitro membrane fragments from the striatum (Guyon et al., 1979; Malfroy et al., 1978; Hiranuma and Oka, 1986; Hiranuma et al., 1997, 1998) but also from what has been seen in other brain regions using cellular readouts of opioid receptor activity. For example, in the locus coeruleus (Williams et al., 1987) and spinal cord (Song and Marvizon, 2003), enkephalin degradation relies on multiple or alternative peptidases. It may be that the differential peptidase activity in membrane fragments arises from the contribution of intracellular peptidases that would not participate in our experiments. However, this cannot explain the difference between the current results and results from experiments using cellular readouts of opioid receptor function (Williams et al., 1987; Song and Marvizon, 2003). We suggest three possible explanations for this difference. Firstly, we suggest that there is heterogenous expression of enkephalin-degrading peptidases in discrete neural circuits. Although there is widespread distribution of all three peptidases in the brain at the macroscopic level, the dominance of NEP in the intercalated cells may result from higher microscopic expression of NEP in amygdala nuclei compared with other brain peptidases. Indeed, immunohistochemical and radiochemical mapping

of NEP in the CNS have shown higher patterns of NEP expression and activity within amygdala nuclei (Waksman et al., 1986; Pollard et al., 1989) compared with only moderate and/or negligible levels of ACE (Strittmatter et al., 1984; Chai et al., 1987) and APN (Noble et al., 2001; Banegas et al., 2005). By contrast, only low to moderate levels of NEP and high levels of ACE and APN have been observed in brain regions such as the locus coeruleus and spinal cord, where enkephalin degradation relies on multiple peptidases (Pollard et al., 1989; Noble et al., 2001; Facchinetti et al., 2003). A second possible explanation is that only synaptic enkephalin concentrations, as measured here, are determined by NEP in the intercalated cells, whereas the other enkephalin-degrading enzymes may contribute to enkephalin breakdown at other cellular locations, such as the cell body or dendrites, or even intracellularly (Williams et al., 1987; Song and Marvizon, 2003). If this is the case, subcellular localization in addition to regional distribution should be considered when elucidating the physiologic control of peptides by peptidases. The third possible explanation for the dominance of NEP in the intercalated cells is more speculative but warrants consideration. As we showed in this study, NEP also controls the synaptic concentrations of N/OFQ in the intercalated cells. Likewise, APN and ACE have a broad substrate specificity and degrade peptides with susceptible peptide bonds, such as substance P (Hooper et al., 1985), neurokinins (Marvizon et al., 2003), angiotensin and bradykinin (Dorer et al., 1974), and cholecystokinin (Matsas et al., 1984). Given this, if any of the other peptides targeted by APN and ACE are present at significant synaptic concentrations in the intercalated cells, they may compete with enkephalin for degradation and thus limit APN and ACE effects. Regardless of the mechanism, these data suggest that the mechanisms by which neuropeptides are metabolized, either in membrane fragments or in other regions of the CNS, cannot be generalized. Thus, to appropriately determine the influence of peptidases over peptide actions in the CNS, tissue from specific regions of interest containing 1) native levels of peptidase activity, 2) intact cellular microarchitecture, and 3) other peptides targeted by the peptidase of interest must be used.

In this study, we examined peptidase control of enkephalin under control conditions. However, many factors can alter peptidase expression and activity, including chronic morphine treatment (Malfroy et al., 1978), stress (Hernández et al., 2009), stroke (Kerridge et al., 2015), and increasing age/Alzheimer disease (Reilly, 2001). Given the location specificity we have defined in this study, it would be interesting to test whether disease pathology changes peptidase activity, and thus peptide level, and whether these changes occur globally or at specific locations. Defining the specific peptidase and how it may change in a disease state would allow rational choices of drugs targeting the specific peptidase of interest. For example, increases in NEP activity within the amygdala could be usefully targeted using currently available drugs to regulate endogenous opioid actions in drug addiction, pain, or fear disorders.

Authorship Contributions

Participated in research design: Gregoriou, Bagley.
Conducted experiments: Gregoriou, Patel, Winters.
Performed data analysis: Gregoriou, Bagley.
Wrote or contributed to writing of manuscript: Gregoriou, Bagley.

References

Banegas I, Prieto I, Alba F, Vives F, Araque A, Segarra AB, Durán R, de Gasparo M, and Ramírez M (2005) Angiotensinase activity is asymmetrically distributed in the amygdala, hippocampus and prefrontal cortex of the rat. *Behav Brain Res* **156**: 321–326.

Barnes K, Matsas R, Hooper NM, Turner AJ, and Kenny AJ (1988) Endopeptidase-24.11 is striosomally ordered in pig brain and, in contrast to aminopeptidase N and peptidyl dipeptidase A ('angiotensin converting enzyme'), is a marker for a set of striatal efferent fibres. *Neuroscience* **27**:799–817.

Bayes-Genis A, Barallat J, and Richards AM (2016) A test in context: neprilysin: function, inhibition, and biomarker. *J Am Coll Cardiol* **68**:639–653.

Bodnar RJ (2018) Endogenous opiates and behavior: 2016. *Peptides* **101**:167–212.

Chai SY, Mendelsohn FA, and Paxinos G (1987) Angiotensin converting enzyme in rat brain visualized by quantitative in vitro autoradiography. *Neuroscience* **20**: 615–627.

Chou J, Tang J, Del Rio J, Yang HY, and Costa E (1984) Action of peptidase inhibitors on methionine5-enkephalin-arginine6-phenylalanine7 (YGGFMRF) and methionine5-enkephalin (YGGFM) metabolism and on electroacupuncture antinociception. *J Pharmacol Exp Ther* **230**:349–352.

Dalkas GA, Marchand D, Galleyrand JC, Martinez J, Spyroulias GA, Cordopatis P, and Cavelier F (2010) Study of a lipophilic captopril analogue binding to angiotensin I converting enzyme. *J Pept Sci* **16**:91–97.

Dorer FE, Kahn JR, Lentz KE, Levine M, and Skeggs LT (1974) Hydrolysis of bradykinin by angiotensin-converting enzyme. *Circ Res* **34**:824–827.

Erdös EG, Johnson AR, and Boyden NT (1978) Hydrolysis of enkephalin by cultured human endothelial cells and by purified peptidyl dipeptidase. *Biochem Pharmacol* **27**:843–848.

Facchinetti P, Rose C, Schwartz JC, and Ouimet T (2003) Ontogeny, regional and cellular distribution of the novel metalloprotease neprilysin 2 in the rat: a comparison with neprilysin and endothelin-converting enzyme-1. *Neuroscience* **118**: 627–639.

Gros C, Giros B, and Schwartz JC (1985) Purification of membrane-bound aminopeptidase from rat brain: identification of aminopeptidase M. *Neuropeptides* **5**: 485–488.

Guyon A, Roques BP, Guyon F, Foucault A, Perdrisot R, Swerts JP, and Schwartz JC (1979) Enkephalin degradation in mouse brain studied by a new H.P.L.C. method: further evidence for the involvement of carboxydipeptidase. *Life Sci* **25**:1605–1611.

Hernández J, Segarra AB, Ramírez M, Banegas I, de Gasparo M, Alba F, Vives F, Durán R, and Prieto I (2009) Stress influences brain enkephalinase, oxytocinase and angiotensinase activities: a new hypothesis. *Neuropsychobiology* **59**:184–189.

Hersh LB (1985) Characterization of membrane-bound aminopeptidases from rat brain: identification of the enkephalin-degrading aminopeptidase. *J Neurochem* **44**: 1427–1435.

Hiranuma T, Iwao K, Kitamura K, Matsumiya T, and Oka T (1997) Almost complete protection from [Met5]-enkephalin-Arg6-Gly7-Leu8 (Met-enk-RGL) hydrolysis in membrane preparations by the combination of amastatin, captopril and phosphoramidon. *J Pharmacol Exp Ther* **281**:769–774.

Hiranuma T, Kitamura K, Taniguchi T, Kobayashi T, Tamaki R, Kanai M, Akahori K, Iwao K, and Oka T (1998) Effects of three peptidase inhibitors, amastatin, captopril and phosphoramidon, on the hydrolysis of [Met5]-enkephalin-Arg6-Phe7 and other opioid peptides. *Naunyn Schmiedebergs Arch Pharmacol* **357**:276–282.

Hiranuma T and Oka T (1986) Effects of peptidase inhibitors on the [Met5]-enkephalin hydrolysis in ileal and striatal preparations of guinea-pig: almost complete protection of degradation by the combination of amastatin, captopril and thiorphan. *Jpn J Pharmacol* **41**:437–446.

Hooper NM, Kenny AJ, and Turner AJ (1985) The metabolism of neuropeptides. Neurokinin A (substance K) is a substrate for endopeptidase-24.11 but not for peptidyl dipeptidase A (angiotensin-converting enzyme). *Biochem J* **231**:357–361.

Inguimbert N, Coric P, Poras H, Meudal H, Teffot F, Fournié-Zaluski MC, and Roques BP (2002) Toward an optimal joint recognition of the S1′ subsites of endothelin converting enzyme-1 (ECE-1), angiotensin converting enzyme (ACE), and neutral endopeptidase (NEP). *J Med Chem* **45**:1477–1486.

Janak PH and Tye KM (2015) From circuits to behaviour in the amygdala. *Nature* **517**:284–292.

Kerridge C, Kozlova DI, Nalivaeva NN, and Turner AJ (2015) Hypoxia affects neprilysin expression through caspase activation and an APP intracellular domain-dependent mechanism. *Front Neurosci* **9**:426.

Kitabgi P, Dubuc I, Nouel D, Costentin J, Cuber JC, Fulcrand H, Doulut S, Rodriguez M, and Martinez J (1992) Effects of thiorphan, bestatin and a novel metallopeptidase inhibitor JMV 390-1 on the recovery of neurotensin and neuromedin N released from mouse hypothalamus. *Neurosci Lett* **142**:200–204.

Krizanová O, Kiss A, Záciková L, and Jezová D (2001) Nitric oxide synthase mRNA levels correlate with gene expression of angiotensin II type-1 but not type-2 receptors, renin or angiotensin converting enzyme in selected brain areas. *Physiol Res* **50**:473–480.

Lutz PE and Kieffer BL (2013) Opioid receptors: distinct roles in mood disorders. *Trends Neurosci* **36**:195–206.

Malfroy B, Swerts JP, Guyon A, Roques BP, and Schwartz JC (1978) High-affinity enkephalin-degrading peptidase in brain is increased after morphine. *Nature* **276**: 523–526.

Marvizon JC, Wang X, Lao LJ, and Song B (2003) Effect of peptidases on the ability of exogenous and endogenous neurokinins to produce neurokinin 1 receptor internalization in the rat spinal cord. *Br J Pharmacol* **140**:1389–1398.

Matsas R, Fulcher IS, Kenny AJ, and Turner AJ (1983) Substance P and [Leu] enkephalin are hydrolyzed by an enzyme in pig caudate synaptic membranes that is identical with the endopeptidase of kidney microvilli. *Proc Natl Acad Sci USA* **80**:3111–3115.

Matsas R, Turner AJ, and Kenny AJ (1984) Endopeptidase-24.11 and aminopeptidase activity in brain synaptic membranes are jointly responsible for the hydrolysis of cholecystokinin octapeptide (CCK-8). *FEBS Lett* **175**:124–128.
Miyamoto A, Murata S, and Nishio A (2002) Role of ACE and NEP in bradykinin-induced relaxation and contraction response of isolated porcine basilar artery. *Naunyn Schmiedebergs Arch Pharmacol* **365**:365–370.
Neal CR Jr., Mansour A, Reinscheid R, Nothacker HP, Civelli O, and Watson SJ Jr. (1999) Localization of orphanin FQ (nociceptin) peptide and messenger RNA in the central nervous system of the rat. *J Comp Neurol* **406**:503–547.
Noble F, Banisadr G, Jardinaud F, Popovici T, Lai-Kuen R, Chen H, Bischoff L, Parsadaniantz SM, Fournie-Zaluski MC, and Roques BP (2001) First discrete autoradiographic distribution of aminopeptidase N in various structures of rat brain and spinal cord using the selective iodinated inhibitor [^{125}I]RB 129. *Neuroscience* **105**:479–488.
Pollard H, Bouthenet ML, Moreau J, Souil E, Verroust P, Ronco P, and Schwartz JC (1989) Detailed immunoautoradiographic mapping of enkephalinase (EC 3.4.24.11) in rat central nervous system: comparison with enkephalins and substance P. *Neuroscience* **30**:339–376.
Reilly CE (2001) Neprilysin content is reduced in Alzheimer brain areas. *J Neurol* **248**:159–160.
Rich DH, Moon BJ, and Harbeson S (1984) Inhibition of aminopeptidases by amastatin and bestatin derivatives. Effect of inhibitor structure on slow-binding processes. *J Med Chem* **27**:417–422.
Roques BP, Fournié-Zaluski MC, Soroca E, Lecomte JM, Malfroy B, Llorens C, and Schwartz JC (1980) The enkephalinase inhibitor thiorphan shows antinociceptive activity in mice. *Nature* **288**:286–288.
Rose C, Voisin S, Gros C, Schwartz JC, and Ouimet T (2002) Cell-specific activity of neprilysin 2 isoforms and enzymic specificity compared with neprilysin. *Biochem J* **363**:697–705.
Sakurada C, Sakurada S, Orito T, Tan-No K, and Sakurada T (2002) Degradation of nociceptin (orphanin FQ) by mouse spinal cord synaptic membranes is triggered by endopeptidase-24.11: an in vitro and in vivo study. *Biochem Pharmacol* **64**: 1293–1303.
Schwartz J, Costentin J, and Lecomte J (1985) Pharmacology of enkephalinase inhibitors. *Trends Pharmacol Sci* **6**:472–476.
Schwartz JC, Gros C, Lecomte JM, and Bralet J (1990) Enkephalinase (EC 3.4.24.11) inhibitors: protection of endogenous ANF against inactivation and potential therapeutic applications. *Life Sci* **47**:1279–1297.
Song B and Marvizón JCG (2003) Peptidases prevent μ-opioid receptor internalization in dorsal horn neurons by endogenously released opioids. *J Neurosci* **23**:1847–1858.
Strittmatter SM, Lo MM, Javitch JA, and Snyder SH (1984) Autoradiographic visualization of angiotensin-converting enzyme in rat brain with [^{3}H]captopril: localization to a striatonigral pathway. *Proc Natl Acad Sci USA* **81**:1599–1603.
Sullivan S, Akil H, and Barchas JD (1978) In vitro degradation of enkephalin: evidence for cleavage at the Gly-Phe bond. *Commun Psychopharmacol* **2**:525–531.
Waksman G, Hamel E, Delay-Goyet P, and Roques BP (1986) Neuronal localization of the neutral endopeptidase 'enkephalinase' in rat brain revealed by lesions and autoradiography. *EMBO J* **5**:3163–3166.
Whyteside AR and Turner AJ (2008) Human neprilysin-2 (NEP2) and NEP display distinct subcellular localisations and substrate preferences. *FEBS Lett* **582**: 2382–2386.
Williams JT, Christie MJ, North RA, and Roques BP (1987) Potentiation of enkephalin action by peptidase inhibitors in rat locus ceruleus in vitro. *J Pharmacol Exp Ther* **243**:397–401.
Winters BL, Gregoriou GC, Kissiwaa SA, Wells OA, Medagoda DI, Hermes SM, Burford NT, Alt A, Aicher SA, and Bagley EE (2017) Endogenous opioids regulate moment-to-moment neuronal communication and excitability. *Nat Commun* **8**: 14611.

Address correspondence to: E.E. Bagley, Discipline of Pharmacology & Charles Perkins Centre, Charles Perkins Centre D17, University of Sydney, Camperdown, NSW, 2006, Australia. E-mail: elena.bagley@sydney.edu.au